From one-dimensional charge conserving superconductors to the gapless Haldane phase

Anna Keselman,[1,2] Erez Berg,[3,2] and Patrick Azaria[4,2]
[1]*Station Q, Microsoft Research, Santa Barbara, California 93106-6105, USA*
[2]*Department of Condensed Matter Physics, Weizmann Institute of Science, Rehovot, Israel 7610001*
[3]*James Frank Institute, The University of Chicago, Chicago, Illinois 60637, USA*
[4]*Laboratoire de Physique Thorique des Liquides, Universit Pierre et Marie Curie, 4 Place Jussieu, 75252 Paris, France*

(Received 24 February 2018; revised manuscript received 29 June 2018; published 3 December 2018)

We develop a framework to analyze the topological properties of one-dimensional systems with charge conservation and tendency towards topological superconducting order. In particular, we consider models with N flavors of fermions and $(\mathbb{Z}_2)^N$ symmetry, associated with the conservation of the fermionic parity of each flavor. For $N = 1$, and with no other symmetry other than charge conservation, we recover the result that there is no distinct topological phase with exponentially localized zero modes. For $N > 1$, however, we show that the ends of the system can host low-energy, exponentially-localized modes. To illustrate these ideas, we focus on lattice models with $SO(N)$ symmetric interactions and study the phase transition between the trivial and the topological gapless phases using bosonization and a weak-coupling renormalization group analysis. As a concrete example, we study in detail the case of $N = 3$. In this case, the topologically nontrivial superconducting phase corresponds to a gapless analog of the Haldane phase in spin-1 chains. In this phase, although the bulk hosts *gapless* modes, corresponding to composite fermionic excitations with an enlarged Fermi surface, the ends host spin-1/2 degrees of freedom which are exponentially localized and protected by the spin gap in the bulk. We obtain the full phase diagram of the model using density matrix renormalization group calculations. Within this model, we identify the self-dual line studied by Andrei and Destri [Nucl. Phys. B **231**, 445 (1984)] as a first-order transition line between the gapless Haldane phase and a trivial gapless phase. This allows us to identify the propagating spin-1/2 kinks in the Andrei-Destri model as the topological end modes at the domain walls between the two phases.

DOI: 10.1103/PhysRevB.98.214501

I. INTRODUCTION

One-dimensional topological superconductors have been in the focus of both experimental and theoretical study in condensed matter physics in the past decade, due to the unique excitations, Majorana bound states, they host at their ends [1–3]. The topological protection of these modes relies on the bulk of the system being gapped. This is the case if the one-dimensional system is proximity coupled to a bulk superconductor. However, in a purely one-dimensional system, in which superconductivity arises from intrinsic attractive pairing interactions, the bulk of the system remains gapless due to large quantum phase fluctuations.

In spin-polarized systems with intrinsic pairing interactions, Majorana end modes are, generically, no longer protected [4,5] since the bulk is gapless to single particle excitations [6,7]. In this work, we discuss situations where well-defined, exponentially localized end modes can survive in a purely one-dimensional system in the presence of additional symmetries. Several examples of such phases are known [8–17]. However, a general framework that relates these phases to their noncharge conserving (mean field) counterparts has not been given.

Here, we develop a general approach to treat one-dimensional systems with multiple fermion flavors and intrinsic, charge-conserving, attractive interactions. As a test case, we study a family of models with $(\mathbb{Z}_2)^N$ symmetry, associated with the conservation of the fermionic parity of each flavor. We show how the result for the spinless case ($N = 1$) can be recovered using this approach. We then address the case of $N > 1$ flavors and show that in this case, the system can host low-energy exponentially localized end modes, reminiscent of the Majorana zero modes, despite the gaplessness of the bulk.

We discuss the low-energy structure of the gapless topological phases for arbitrary N and emphasize the connection between the nature of the low-energy modes in the bulk and the protection of the end modes. We show that for odd N, the bulk hosts low-energy composite fermionic excitations, with momentum Nk_F. For even N the bulk hosts only bosonic excitations.

Further, we present a more detailed analysis of lattice models with $SO(N)$ symmetric interactions. In this case, the protection of the end modes can be understood as arising from the presence of a spin gap in the bulk. For $N = 2$, we recover the phase studied previously in Refs. [12,18,19], where it was shown that the protection is in fact robust to breaking of $SO(2)$ symmetry, as long as time-reversal symmetry is present. For $N = 3$, we show that the topological superconducting phase is closely related to the Haldane phase in spin-1 chains. In this phase, although the bulk is gapless to single particle excitations, the ends host spin-1/2 degrees of freedom which are exponentially localized and protected by a spin gap in the bulk [20].

This paper is organized as follows. We start by presenting the model under consideration in Sec. II, discussing the connection to fully-gapped topological superconductors and

addressing the stability of the topological phase to quantum phase fluctuations based on general heuristic arguments. We explain the connection between the nature of the bulk low-energy modes and the topological protection of the end modes. In Sec. III, we analyze the low-energy physics of the gapless topological phase in greater detail, distinguishing between the cases of even and odd N. In Sec. IV, we focus on $SO(N)$ symmetric models. We present a field theory analysis backing up the heuristic arguments presented previously. To this end, we discuss a slightly generalized model with on-site interactions, which hosts both a trivial and a topological gapless phase. We discuss a duality transformation relating these phases and the phase diagram expected from weak coupling RG. In Sec. V we study in detail the lattice model for $N = 3$, with both on-site and nearest-neighbors $SO(3)$ symmetric pairing interactions, and map out its phase diagram using the density matrix renormalization group (DMRG) [21,22]. The topological superconducting phase in this model is identified as a gapless analog of the symmetry-protected Haldane phase of $S = 1$ spin chains. The conclusions are summarized in Sec. VI.

II. STABILITY OF TOPOLOGICAL SUPERCONDUCTORS IN 1D CHARGE CONSERVING SYSTEMS

We start by describing a general heuristic argument to analyze the stability of topological phases in one-dimensional charge-conserving superconductors and their protected edge modes.

A. Spinless wire

Consider a one-dimensional system of spinless fermions with a general short-range Hamiltonian that conserves the total charge. If the density of particles is incommensurate with the lattice (i.e., the number of particles per unit cell is irrational), the system is generally gapless [23]. Our goal is to map the possible distinct phases of the system and to understand their low-energy properties; in particular, we ask about the nature of low-energy gapless modes in the bulk and whether there are any well-defined zero modes bound to the edges.

The problem of a single "flavor" of fermions with no symmetries other than charge conservation has been analyzed by various authors [4,5,10,24]; in this case, two distinct gapless phases are possible, one with a gap to single fermions in the bulk (but no gap to pairs of fermions) and the other with no gap to single fermions. Neither of these phases supports exponentially localized edge modes. Below, we derive this result using a general, heuristic argument; the argument is then easy to generalize to systems with additional symmetries.

For concreteness, it is useful to consider the following simple Hamiltonian of spinless fermions on a one-dimensional lattice:

$$H = \sum_i (-t c_i^\dagger c_{i+1} + \text{H.c.} - \mu c_i^\dagger c_i) + \sum_{i,j} V_{ij} \Pi_i^\dagger \Pi_j, \quad (1)$$

where c_i ($c_i^\dagger$) is the annihilation (creation) operator of a fermion on site i, t is the nearest neighbor hopping amplitude, μ is the chemical potential, $\Pi_i^\dagger = c_i^\dagger c_{i+1}^\dagger$, and $V_{ij} < 0$ denotes the strength of attractive interactions. We will assume that the interactions are short-ranged, i.e., decay sufficiently fast (faster than any power law) at large distances but not necessarily nearest neighbor. Our considerations will be much more general and apply to any one-dimensional Hamiltonian of spinless fermions (including further neighbor hopping, other forms of interactions, etc.).

We formulate the problem as a path integral and decouple the interaction term via a Hubbard-Stratonovich transformation

$$Z = \int \prod_i Dc_i D\bar{c}_i D\Delta_i e^{-\int d\tau L}, \quad (2)$$

where $c_i, \bar{c}_i$ are Grassmann variables and the Lagrangian is given by

$$L = -\sum_i \bar{c}_i(\partial_\tau - \mu)c_i + \sum_i (-t\bar{c}_i c_{i+1} + \Delta_i \bar{c}_i \bar{c}_{i+1} + \text{H.c.}) + \sum_{i,j} (V^{-1})_{ij} \Delta_i \Delta_j^*. \quad (3)$$

We assume fluctuations in the amplitude of Δ_i are small and denote $\Delta_i = |\Delta| e^{2i\theta_i}$. The last term in (3) gives rise to a finite phase stiffness of θ, allowing us to assume that it changes slowly between neighboring sites. Hereafter, we assume the phase varies slowly but omit this term for simplicity.

If the attractive interactions are sufficiently strong and long-ranged, i.e., if the interactions extend over a finite but large distance, then the phase $\theta_i(\tau)$ fluctuates slowly in space and time. Approaching the problem from this quasiordered limit, we introduce neutral fermions $f_i = c_i e^{-i\theta_i}$. (Note that under a $U(1)$ gauge transformation $c_i \to c_i e^{i\alpha}$, $\theta_i \to \theta_i + \alpha$ leaving the f_i fermions unchanged.) Since the phase varies little on the scale of a lattice spacing, the pairing and hopping terms can be approximated as $\Delta_i \bar{c}_i \bar{c}_{i+1} = \Delta \bar{f}_i \bar{f}_{i+1} e^{i(\theta_i - \theta_{i+1})} \approx \Delta \bar{f}_i \bar{f}_{i+1}$ and $t\bar{c}_i c_{i+1} = t e^{i(\theta_{i+1} - \theta_i)} \bar{f}_i f_{i+1} \approx t \bar{f}_i f_{i+1}$.

Special care needs to be taken when considering the boundary conditions of the f_i fermions on a closed ring. Phase configurations where the phase θ_i winds by $n_\theta \pi$, where $n_\theta \in \mathbb{Z}$ (i.e., $\theta_{N_x} \approx \theta_1 + n_\theta \pi$, where N_x is the number of sites) should be accounted for. To avoid a discontinuity in the parameters of the Hamiltonian across the bond from site N_x to 1, we can encode the winding number in the boundary conditions of the fermions: $f_{N_x+1} = (-1)^{n_\theta} f_1$.

After the transformation to the f_i fermions, and assuming a nearly-static phase configuration, the Lagrangian is written as:

$$L = \sum_i [\bar{f}_i(\partial_\tau - \mu) f_i + i n_i \partial_\tau \theta_i] + \sum_i (-t \bar{f}_i f_{i+1} + \Delta \bar{f}_i \bar{f}_{i+1} + \text{H.c.}), \quad (4)$$

where $n_i = f_i^\dagger f_i = c_i^\dagger c_i$ is the occupation of site i, and the boundary conditions of the fermions are periodic (antiperiodic) if the winding number of the phase is even (odd), respectively. Hence, the problem of finding the phase structure of the Hamiltonian (1) has been mapped to the problem of classifying the possible phases of the f fermions that

obey a mean-field-like static Hamiltonian with a dynamically determined boundary condition.

For $-2t < \mu < 2t$, the f fermions realize a nontrivial, class-D [25] topological superconductor, i.e., a Kitaev chain. However, we argue below that the topological properties of the phase (and in particular, its protected zero modes) are lost due to the coupling between the f fermions and the phase winding of the superconducting order parameter, n_θ. This coupling allows for low-energy single particle excitations in the bulk of the system, unlike the mean-field case, where single fermions are gapped in the bulk. Such excitations can couple between the Majorana modes at the ends of the chain, removing the exponential ground state degeneracy.

To see that the bulk is gapless to single particle excitations consider a system with periodic boundary conditions and $\mathcal{N}$ fermions. Recall that a Kitaev chain on a closed ring has a unique ground state with a well defined fermion parity [26]. Adding a single fermion excites the system to energy Δ, the magnitude of the superconducting gap. However, in our case, this gap can be avoided by introducing a π phase winding in θ, changing the boundary conditions of the f fermions from periodic to antiperiodic or vice versa. The Kitaev chain's ground state has an opposite fermion parity with periodic and antiperiodic boundary conditions [26]. Therefore, the energy cost of adding a single fermion is only due to the extra phase winding (which costs an energy proportional to the inverse of the system size; this is nothing but the charging energy). Due to the presence of low energy single fermion excitations in the bulk, the end modes are no longer exponentially localized; they can leak into the bulk and the localization becomes power law, with a power dictated by the Luttinger parameter in the wire [4,5].

If the f fermions in (4) realize a trivial superconducting phase, the superconducting gap Δ cannot be avoided when an extra fermion is added to the system, since changing the boundary conditions no longer changes the fermion parity of the ground state. Hence, the bulk is gapped to single particle excitations. However, in this case there are no low-energy end modes. This establishes that the single-flavor chain ($N = 1$) supports two distinct phases, as has been discussed in Refs. [7,24], neither of which supports exponentially localized end modes.

The same conclusion can be reached from a bosonization analysis. The system in this case maps to a single-flavor Luttinger liquid which has no gap to single fermions. However, the argument above is more general: It implies that, as a matter of principle,[1] a topological phase with a single Majorana end mode cannot be stable if charge is conserved, since the bulk must be gapless to single fermion excitations.

B. Wire with N flavors

Let us now study a less trivial situation where several flavors of fermions are present. We shall consider a model with N flavors, $c_{a=1,\ldots,N}$, each with a Hamiltonian of the form of Eq. (1), and such that the different flavors are coupled only by a pair hopping term. The total Hamiltonian is given by

$$H = \sum_{a=1}^{N} H_a + H_{\text{int}}, \tag{5}$$

where

$$\begin{aligned} H_a &= \sum_i (-t c^\dagger_{i,a} c_{i+1,a} + \text{H.c.} - \mu c^\dagger_{i,a} c_{i,a}) \\ &\quad + \sum_{i,j} V^a_{ij}\ \Pi^\dagger_{i,a} \Pi_{j,a}, \\ H_{\text{int}} &= \sum_{i,j,a,b} V^{ab}_{ij}\ \Pi^\dagger_{i,a} \Pi_{j,b}, \end{aligned} \tag{6}$$

where $\Pi^\dagger_{i,a} = c^\dagger_{i,a} c^\dagger_{i+1,a}$ is a p-wave pair creation operator for a single flavor and $V^a_{ij} < 0$ denotes the attractive interaction within each flavor channel. The pair hopping couplings, $V^{ab}_{ij} = V^{ba}_{ij}$, are assumed to be short ranged. We shall also restrict ourselves to attractive interactions $V^{ab}_{ij} < 0$.

The Hamiltonian (6) has a global $U(1)$ symmetry associated with total charge conservation and a $(\mathbb{Z}_2)^N$ symmetry associated with the conservation of the fermionic parity of each flavor. Introducing the fermionic parity operator associated with a flavor a,

$$P_a = (-1)^{n_a}, \quad n_a = \sum_i c^\dagger_{i,a} c_{i,a}, \tag{7}$$

we see indeed that $[P_a, H] = 0$, $a = (1, \ldots, N)$. The above symmetry is of utmost importance in regards to the topological properties of (6). Indeed, as shown in Ref. [5], if not for the above $(\mathbb{Z}_2)^N$ symmetry, the topological character of the N Kitaev chains would not survive when charge conservation is imposed. As we shall argue below, the $(\mathbb{Z}_2)^N$ symmetry (7) protects the end modes associated with each chain from leaking into the bulk and allows, even in a charge conserving system, for symmetry protected topological (SPT) phases for all $N > 1$. In Sec. V we will consider a concrete model in which this symmetry arises naturally as a subgroup of the SO(3). Below, we will only assume that the $(\mathbb{Z}_2)^N$ symmetry (7) is present and keep the discussion as general as possible, allowing $V^a_{ij} < 0$ and $V^{ab}_{ij} < 0$ to be arbitrary.

1. Bulk spectrum

Following the same procedure as in Sec. II A, we introduce Hubbard-Stratonovich fields $\Delta_{i,a} = |\Delta_{i,a}| e^{2i\theta_{i,a}}$ and neutral fermions $f_{i,a} = c_{i,a} e^{-i\theta_{i,a}}$. We neglect the amplitude fluctuations of the superconducting order parameters, replacing $|\Delta_{i,a}|$ by $\Delta_a > 0$. The Lagrangian takes the form

$$L = \sum_{a=1}^{N} L_a + L_{\text{int}}, \tag{8}$$

where L_a is the Lagrangian associated with a single Kitaev chain of flavor a

$$\begin{aligned} L_a &= \sum_i [\bar{f}_{i,a}(\partial_\tau - \mu) f_{i,a} + i n_{i,a} \partial_\tau \theta_{i,a}] \\ &\quad + \sum_i (-t\, \bar{f}_{i,a} f_{i+1,a} + \Delta_a\ \bar{f}_{i,a} \bar{f}_{i+1,a} + \text{H.c.}), \end{aligned} \tag{9}$$

[1] This conclusion does not rely on any particular field theoretic formulation; it follows directly from the action (4).

and

$$L_{\rm int} = \sum_{i,j} \sum_{a \neq b} J_{ij}^{ab} \cos 2(\theta_{i,a} - \theta_{j,b}), \tag{10}$$

where $J_{ij}^{ab} = 2\Delta_a \Delta_b (V_{ij}^{ab} + V_{ij}^{a} \delta_{ab})^{-1}$ are Josephson couplings which tend to lock the phases $\theta_{i,a}$ together. As in the single-flavor case, on a ring with N_x sites, the fermions satisfy the boundary conditions: $f_{N_x+1,a} = (-1)^{n_{\theta,a}} f_{1,a}$, where $n_{\theta,a}$ is the winding number of the superconducting phase of flavor a: $\theta_{N_x,a} \approx \theta_{1,a} + n_{\theta,a}\pi$ [see discussion above Eq. (4)].

Assuming that the phases $\theta_{i,a}$ are slowly varying, one may integrate out the f fermions. In the low-energy limit the Lagrangian (8) reduces to [5]

$$L = \int dx \sum_{a=1}^{N} \frac{K_a}{2\pi} \left(\frac{1}{v_a} (\partial_\tau \theta_a)^2 + v_a (\partial_x \theta_a)^2 \right) + \int dx \sum_{a \neq b = 1}^{N} G^{ab} \cos 2(\theta_a(x) - \theta_b(x)), \tag{11}$$

where θ_a is the phase field of flavor a, K_a is the Luttinger parameter associated with the flavor, v_a is the respective velocity, and $G^{ab} < 0$ are effective Josephson couplings that lock the phases to each other such that $\theta_a(x) - \theta_b(x) = (p_a - p_b)\pi$, $p_a \in \mathbb{Z}$.

Consider now adding a single fermion of a given flavor to a system on a ring. As in the spinless case analyzed above, the energy cost of adding a single fermion of flavor a can be avoided by introducing a phase winding in the field θ_a. However, as the phases $\theta_{1,\ldots,N}$ are now locked to each other by the Josephson couplings (10), such a phase winding costs a finite energy Δ_σ. We conclude, therefore, that for $N > 1$ there is a gap to adding a fermion of a single flavor. The same reasoning can be applied to excitations involving adding or removing M fermions of different flavors and leads to the conclusion that they are all gapped unless $M = N$.

An excitation involving adding (or removing) a single fermion of *each* flavor, however, is gapless (i.e., costs energy proportional to the inverse of the system size). To see this, consider introducing a phase winding *simultaneously* in all the fields θ_a, thus avoiding the spin gap Δ_σ. Doing so switches the boundary conditions of fermions of all the flavors f_a, while at the same time the fermionic parities of all N flavors are changed, $P_a \to -P_a$ $(a = 1, \ldots, N)$, thus avoiding the superconducting gap Δ_a in each chain. The only energy cost then is due to the phase twist which scales as $1/L$.

We therefore conclude that there are two types of gapless excitations in the system. Gapless excitations of the first type involve adding (or removing) pairs of fermions of the *same* flavor, without changing the fermionic parity of any flavor (e.g., by acting with the p-wave creation operator $\Pi_{i,a}^\dagger$). Excitations of the second type are composite operators involving N fermions of *different* flavors that change the parity of all flavors. In this respect the composite operators

$$\tilde{c}_{i,Q}^\dagger \sim c_{i,a_1}^\dagger \ldots c_{i,a_M}^\dagger c_{i,b_1} \ldots c_{i,b_{N-M}}, \tag{12}$$

which have charge $Q = 2M - N$, have a finite overlap with the gapless modes of the system. These composite excitations are fermionic for N odd and bosonic for N even. As a consequence, when N is even the low-energy excitations are always bosonic whereas, when N is odd, there exist both fermionic and bosonic excitations: While the fermions change the fermionic parity of all flavors, the bosons do not.

2. End modes

Let us now investigate the fate of the end modes in a system with N flavors, in light of the preceding discussion. If we neglect the fluctuations of the phase in the action of the f_a fermions [Eq. (10)] then for $-2t < \mu < 2t$, each flavor hosts a pair of zero-energy Majorana modes, $\gamma_{L,a}$ and $\gamma_{R,a}$, localized at the two ends of an open chain. We shall argue that the low-energy excitations in the bulk cannot couple the zero modes of the two edges; therefore, a system with open boundary conditions has exponentially localized edge modes, even when the phase fluctuations are taken into account.

To see this, recall that the operators that create gapless bulk excitations either preserve the fermionic parity of each flavor separately, or change the fermionic parity of *all* flavors. In the first case, their action on the low-energy Hilbert space associated with each edge has to be proportional to the identity operator, since any nontrivial product of $\gamma_{L(R),a}$'s that act on the left (right) edge changes the parity of at least one flavor. Operators of the form (12), that change the fermionic parity of all the flavors, must act on the low-energy Hilbert space of the left (right) edge as $\Pi_{a=1}^N \gamma_{L(R),a}$. Hence, the coupling between the two ends is necessarily proportional to total fermionic parity:

$$P = \Pi_{a=1}^N P_a = \Pi_{a=1}^N (-i \gamma_{L,a} \gamma_{R,a}). \tag{13}$$

Consequently, this coupling does not lift the topological degeneracy within a given parity sector.

Finally, we discuss the topological degeneracy associated with the edge modes. As usual, we label the states associated with the edges by the occupation number of the complex (Dirac) fermions $d_a = (\gamma_{L,a} + i\gamma_{R,a})/2$. These states can be separated into two sets of 2^{N-1} states of even and odd total fermionic parity. In a system with overall conservation of the number of fermions, states with opposite fermionic parity must also have different charges; therefore, we conclude that the only effect of charge conservation on the low-energy part of the spectrum is to lift the degeneracy between the even and odd parity states by an amount proportional to the charging energy of the system, which scales like $1/L$. The low-energy manifold in each charge sector contains 2^{N-1} states whose energy separation is exponentially small in the size of the system.

The Majorana zero modes at each edge satisfy the Clifford algebra, $\{\gamma_{L,a}, \gamma_{L,b}\} = 2\delta_{a,b}$ and $\{\gamma_{R,a}, \gamma_{R,b}\} = 2\delta_{a,b}$. Therefore, the low-energy Hilbert space of each edge can be described as a $SO(N)$ spinor, $|\alpha_L\rangle$ and $|\alpha_R\rangle$. When N is odd, there is a single irreducible spinor representation $\alpha_{L(R)}$ of dimension $2^{(N-1)/2}$ of the $SO(N)$ group generated by

$$S_{L(R),ab} = \frac{1}{4i} [\gamma_{L(R),a}, \gamma_{L(R),b}], \tag{14}$$

and, in a given parity sector, the 2^{N-1} topological degeneracy is exhausted by the tensor product states $|\alpha_L\rangle \otimes |\alpha_R\rangle$. When N is even the situation is more subtle. Now, there

are two irreducible spinor representations of (14) of dimension $2^{N/2-1}$. The spinors that belong to the two representations, $|\alpha_{L(R),\pm}\rangle$, are eigenvectors of the edge fermionic parity operators $P_{L(R)} = (-i)^{N/2}\Pi_{a=1}^{N}\gamma_{L(R),a}$: $P_{L(R)}|\alpha_{L(R),\pm}\rangle = \pm|\alpha_{L(R),\pm}\rangle$. For N even, the fermionic parity operator (13) can be written as $P = (-1)^{N/2}P_L P_R$ with $[P_L, P_R] = 0$. Therefore, the low energy subspace in a given parity sector is spanned by the tensor products $|\alpha_{L,\pm}\rangle \otimes |\alpha_{R,\pm}\rangle$ for $N/2$ even and $|\alpha_{L,\pm}\rangle \otimes |\alpha_{R,\mp}\rangle$ for $N/2$ odd.

Topological phases of charge-conserving 1D superconductors in other symmetry classes can be understood in a similar way to the arguments laid out above. For example, in class DIII (time reversal with $\mathcal{T}^2 = -1$) [25], the f fermions carry spin 1/2. The f fermions then form one of the two distinct phases of mean-field Hamiltonians in class DIII. In either phase, twisting the boundary conditions does change the fermion parity of the ground state; therefore, there is a gap to single fermions in the bulk. However, in the topological phase each edge supports a topologically protected Kramers' pair, where the two states have an opposite local fermion parity [12].

III. LOW-ENERGY DESCRIPTION OF THE TOPOLOGICAL PHASE

As seen in the above discussion, the stability of the topological phase is ensured by both the $(\mathbb{Z}_2)^N$ symmetry and the particular nature of the gapless modes of the system: The fact that the operators that create these modes are either even under the fermionic parities of all the flavors or odd under all of them is essential in protecting the zero modes at the ends. We now turn to the more familiar description in terms of the effective low-energy bosonized theory, making contact with the considerations above.

As before, we assume that in the low-energy limit the phases associated with different flavors are locked together. Denoting the collective phase by $\Theta(x,\tau)$ the effective low-energy Lagrangian of the system is that of a generalized Luttinger liquid [27]

$$L_{\text{Lutt}} = \frac{K}{2\pi}\int dx\,\left(\frac{1}{v}(\partial_\tau\Theta)^2 + v(\partial_x\Theta)^2\right), \tag{15}$$

where K is the Luttinger parameter and v is the charge velocity. As the Θ field in (15) is conjugate to the total density of particles, $\rho(x) = \sum_{a=1}^{N}\rho_a(x)$,

$$[\rho(x), \Theta(y)] = i\delta(x-y), \tag{16}$$

we define the dual field $\Phi(x)$, as $\rho(x) \equiv \partial_x\Phi(x)$, with $[\Phi(x), \Theta(y)] = iY(y-x)$, $Y(u)$ being the Heaviside step function. The $\Phi(x)$ and $\Theta(x)$ fields are related to the flavor bosonic fields, $\phi_a(x)$ and $\theta_a(x)$, associated with the Luttinger liquids describing each flavor (12) by the canonical transformation

$$\Theta = \frac{1}{N}\sum_{a=1}^{N}\theta_a, \quad \Phi = \sum_{a=1}^{N}\phi_a. \tag{17}$$

These fields are related to the total charge Q and current J,

$$J = \frac{N}{\pi}\int_0^L dx\;\partial_x\Theta, \quad Q = \int_0^L dx\;\partial_x\Phi. \tag{18}$$

We therefore find that the total current of the system is quantized in units of N. As we show below, this is a consequence of both the presence of a flavor gap and of the topological nature of the phase.

The gapless excitations of the generalized Luttinger liquid (15) can be expressed in terms of the vertex operators

$$V_{n,m}(x) \propto e^{i[n\Theta(x)+m\pi\Phi(x)]}, \tag{19}$$

which have the scaling dimension $\Delta_{nm} = (n^2/K + m^2K)/4$. They carry charge and current

$$Q = n, \;\; J = mN, \;\; (n,m) \in \mathbb{Z}, \tag{20}$$

which owing to the relation between current and momentum have momentum $P = Jk_F = mNk_F$, where k_F is the Fermi momentum of the noninteracting fermions c_a. In a Luttinger liquid, the integers (n,m) are not arbitrary and depend on the boundary conditions. For instance, in a system with periodic boundary conditions, the total charge Q and current J carried by an excitation are such that $Q \pm J$ is even,[2] which translates in the present case to

$$n \pm mN \text{ even}, \;\; (n,m) \in \mathbb{Z}. \tag{21}$$

We now observe that, due to (16), the vertex operator $e^{i\pi\Phi(x)}$ introduces a π kink in the phase Θ and hence from (17) it creates π kinks in the phases of all the flavors, θ_a. We therefore conclude that switching the parity of all N chains simultaneously results in inserting a current N. We may now read off from (21) the nature of the massless excitations in the system. When N is even there are only bosonic excitations with even charges $n = 2p$. These excitations may or may not change the fermionic parity of all the flavors depending on the parity of m. When N is odd, fermionic excitations with odd charges, e.g., $n = 2p+1$, necessarily change the fermionic parity of all the flavors since from (21) m is odd. In contrast, bosonic excitations with even charges, e.g., $n = 2p$, must be accompanied by an even number m of π kinks which do not change the fermionic parity of the flavors. We thus recover the results discussed in Sec. II B.

A. N odd and composite fermionic excitations

When N is odd the excitations are either fermionic, for n odd, or bosonic, for n even. The fundamental excitation in this case is the charge $Q = 1$ fermion created by [see Eq. (12)]

$$\Psi_F^\dagger(x) \propto c_{j,a_1}^\dagger \ldots c_{j,a_{(N+1)/2}}^\dagger c_{j,b_1}\ldots c_{j,b_{(N-1)/2}}, \tag{22}$$

where $x = ja_0$, a_0 being the lattice spacing, and j is an integer denoting the lattice site. This operator has a finite overlap with the vertex operators (19). For instance, to leading order we have

$$\Psi_F^\dagger(x) \sim \Psi_L^\dagger\, e^{iNk_Fx} + \Psi_R^\dagger\, e^{-iNk_Fx}, \tag{23}$$

where $\Psi_{L/R}^\dagger \propto e^{i[\Theta(x)\pm\pi\Phi(x)]}$ creates a charge one fermion with left and right moving excitations at momenta $\pm Nk_F$.

[2]This is due to the fact that only operators for which $m+n$ is even are expressible as a combination of electron and hole operators and are hence local in space.

The charge-1 fermion (22) can hence be interpreted as a spinless fermion with an enlarged Fermi surface at $\pm Nk_F$. Furthermore, as discussed in Ref. [27], the system may be viewed as a fermionic Luttinger liquid made of interacting composite fermionic particles with Luttinger parameter K. In this respect notice that when $N = 1$, the composite fermionic particle is identical to the bare fermion, and one recovers the usual Luttinger liquid description.

At this point it is worth stressing that although, when N is odd, the low-energy physics is described by interacting spinless charge-1 fermions, the generalized Luttinger liquid state for $N > 1$ is different from that of a single flavor system. In particular, when expressed in terms of the lattice fermions, the quantum numbers of the low-energy excitations are different, as can be seen from (21), as well as their momentum scale which is Nk_F. They do, however, share an essential feature in that there is no gap to $Q = 1$ fermionic excitations. Hence, the superconducting character of the phase for N odd is to be understood as a phase where the p-wave pair correlation function decays slower at large distances than any other correlation function, despite having no gap to adding single fermions.

Consider for instance the pair creation operator

$$\Pi_a^\dagger(x) = c_{j,a}^\dagger c_{j+1,a}^\dagger \propto e^{2i\Theta(x)}. \tag{24}$$

As we have $\langle \Psi_F^\dagger(x)\Psi_F(0)\rangle \sim x^{-(K+K^{-1})/2}$ and $\langle \Pi_a^\dagger(x)\Pi_a(0)\rangle \sim x^{-2/K}$, the pair correlations dominate for $K > 1/\sqrt{3}$.

Both the composite fermionic operator and the pair creation operators have subdominant components at the higher momenta $P = (2p+1)Nk_F$ and $P = 2pNk_F$. These are generated by the charge neutral operator $e^{2i\pi\Phi(x)}$ which introduces a 2π kink in the Θ field and hence does not change the boundary conditions of the f fermions. The latter operator corresponds to the Nth moment of the density operator [23]

$$\begin{aligned}\rho_N(x) &\sim c_{j,1}^\dagger ... c_{j,N}^\dagger c_{j,1} ... c_{j,N} \\ &\propto e^{2i\pi\Phi(x)+2iNk_Fx} + \text{H.c.}\end{aligned} \tag{25}$$

For instance, the density operator $\rho(x)$, as any other bosonic operator, has only momentum components at $2mNk_F$ and is given to leading order by

$$\rho(x) \sim \bar{\rho} + \partial_x\Phi(x) + A_N e^{2i\pi\Phi(x)+2iNk_Fx} + \text{H.c.}, \tag{26}$$

where A_N is a nonuniversal constant.

B. N even and composite bosonic excitations

Given the constraint (21), when N is even, n has to be even as well, independently of m. Hence, there can only be bosonic excitations and there are no fermionic excitations in the low energy spectrum, contrary to the odd N case. To leading order, the elementary excitation in this case is given by the bosonic vertex operator

$$\Psi_B^\dagger(x) \propto e^{2i\Theta(x)}, \tag{27}$$

which has zero momentum. In terms of the lattice fermions, both the charge $Q = 2$ pair creation operator (23) and the charge $Q = 2$ composite operator (12), with $M = N/2 + 1$, have a finite overlap with (27). This stems from the fact that since N is even, the composite operators (12) always introduce an even number of $\pm\pi$ kinks in the phases θ_a which may average to zero for the mean Θ phase (17). Higher momentum corrections at $P = pNk_F$ to (27) are of course also generated. The charge neutral operator that generates them is $e^{i\pi\Phi(x)}$ which creates a π kink in the phase Θ. In terms of the fermions it is given by the composite density

$$\begin{aligned}\rho_{\frac{N}{2}}(x) &\sim c_{j,a_1}^\dagger ... c_{j,a_{N/2}}^\dagger c_{j,b_1} ... c_{j,b_{N/2}} \\ &\propto e^{i\pi\Phi(x)+iNk_Fx} + \text{H.c.}\end{aligned} \tag{28}$$

We find, in particular, that the total density in this case has momenta components at $\pm Nk_F$

$$\rho(x) \sim \bar{\rho} + \partial_x\Phi(x) + B_N e^{i\pi\Phi(x)+iNk_Fx} + \text{H.c.} \tag{29}$$

IV. SO(N) SYMMETRIC COUPLED CHAINS

We now turn to illustrate the principles we discussed above in a simple lattice model. We shall consider the situation where an $SO(N)$ symmetry is present and set $V_{ij}^{ab} = V_{ij} = V\delta_{i,j}$ in Eq. (6). An on-site repulsive interaction will also be included. The Hamiltonian is given by

$$\begin{aligned}H = &-t\sum_{i,a=1}^{N}(c_{i,a}^\dagger c_{i+1,a} + \text{H.c.}) + V\sum_i \Pi_i^\dagger\Pi_i \\ &+ \frac{U}{2}\sum_i\left(\sum_{a=1}^{N} n_{i,a}\right)^2,\end{aligned} \tag{30}$$

where the operator

$$\Pi_i^\dagger = \sum_{a=1}^{N} c_{i,a}^\dagger c_{i+1,a}^\dagger \tag{31}$$

creates a pair in a $SO(N)$ singlet state and $n_{i,a} = c_{i,a}^\dagger c_{i,a}$ is the density of the fermion of flavor a at site i. In the following we shall assume $V < 0$ and fix the filling to $\bar{n} = 1/N$ for each flavor (one fermion per site). As we show below, the model (30) displays a rich phase diagram, including both insulating and gapless phases, either with or without topologically protected edge modes.

In the following, we shall investigate in more details the physics associated with (30) in the weak-coupling limit, i.e., $|U|/t \ll 1$ and $|V|/t \ll 1$. In Sec. V we will study numerically the case of $N = 3$ in both the strong and the weak coupling limits.

A. Field theory analysis

In the weak-coupling limit, the low-energy physics associated with (30) is obtained in the standard way by linearizing the spectrum around the two Fermi points $\pm k_F$ ($k_F = \pi\bar{\rho}$) associated with the noninteracting fermions. The lattice fermions $c_{j,a}$ are expressed in terms of left and right moving fermionic modes as

$$c_{j,a} \sim \Psi_{L,a}e^{-ik_Fx} + \Psi_{R,a}e^{ik_Fx}, \tag{32}$$

where, similarly to the definitions in the previous section, $x = ja_0$, a_0 being the lattice spacing, and j is an integer. The next

step is to bosonize the fermions, writing $\Psi_{L(R),a}$ as

$$\Psi_{L(R),a}(x) = \frac{\kappa_a}{\sqrt{2\pi a_0}} e^{-i[\theta_a(x) \pm \pi\phi_a(x)]}, \tag{33}$$

where κ_a are Klein factors satisfying $\{\kappa_a, \kappa_b\} = 2\delta_{a,b}$ to ensure fermionic anticommutation relations. The bosonic fields $\phi_a(x)$ and $\theta_b(x)$ satisfy the equal-time commutation relations $[\phi_a(x), \theta_b(y)] = i\delta_{a,b} Y(y-x)$ and are related to the current density, $j_a(x) = \partial_x \theta_a(x)/\pi$, and to the density of each flavor

$$\rho_a(x) \simeq \bar{\rho} + \partial_x \phi_a(x) + \frac{i}{2\pi a_0} e^{2i\pi\phi_a(x) + 2ik_F x} + \text{H.c.}, \tag{34}$$

where $\bar{\rho} = \bar{n}/a_0$. At this point it is convenient to perform a change of basis to the bosonic fields $(\Phi, \vec{\Phi})$ and $(\Theta, \vec{\Theta})$ corresponding to a collective (or charge) mode and to $N-1$ spin modes as follows

$$\begin{aligned} \Phi &= \sum_{a=1}^{N} \phi_a, \quad \vec{\Phi} = \sum_{a=1}^{N} \vec{\omega}_a \phi_a, \\ \Theta &= \frac{1}{N} \sum_{a=1}^{N} \theta_a, \quad \vec{\Theta} = \sum_{a=1}^{N} \vec{\omega}_a \theta_a, \end{aligned} \tag{35}$$

where $\vec{\omega}_{a=1,\ldots,N}$ are $N-1$ components vectors satisfying $\vec{\omega}_a \cdot \vec{\omega}_b = \delta_{a,b} - 1/N$ and $\sum_{a=1}^{N} \vec{\omega}_a = 0$. The latter conditions ensure that the transformation (35) is canonical. For completeness we write also the inverse transformation

$$\begin{aligned} \phi_a &= \Phi/N + \vec{\omega}_a \cdot \vec{\Phi}, \\ \theta_a &= \Theta + \vec{\omega}_a \cdot \vec{\Theta}. \end{aligned} \tag{36}$$

Using these definitions, we find that the low-energy physics of our model is described by the following bosonized Hamiltonian with decoupled spin and charge sectors, $H = H_c + H_s$, where

$$H_c = \frac{v_c}{2\pi} \int dx \left[K(\partial_x \Theta)^2 + \frac{\pi^2}{K} (\partial_x \Phi)^2 \right], \tag{37}$$

and

$$\begin{aligned} H_s = \int dx \Bigg\{ &\frac{v_F}{2\pi} [(\partial_x \vec{\Theta})^2 + \pi^2 (\partial_x \vec{\Phi})^2] + \frac{g_\perp}{2} (\partial_x \vec{\Phi})^2 \\ &- \frac{1}{2\pi^2 a_0^2} \sum_{a<b} [\lambda \cos(2\pi \vec{\alpha}_{ab} \cdot \vec{\Phi}) + \tilde{\lambda} \cos(2\vec{\alpha}_{ab} \cdot \vec{\Theta})] \Bigg\}. \end{aligned} \tag{38}$$

In Eq. (37), $v_F = 2ta_0 \sin(\pi\bar{\rho}a_0)$ is the Fermi velocity of the noninteracting fermions, $K = N/\sqrt{1 + \frac{(N-1)U + \bar{V}}{\pi v_F/a_0}}$, where $\bar{V} = 2V(1 - \cos(2k_F a_0))$, is the charge Luttinger parameter, and $v_c = v_F/K$ is the charge velocity. In the spin sector (38), $\vec{\alpha}_{ab} = \vec{\omega}_a - \vec{\omega}_b$ and the couplings, $\lambda = (g_\parallel + g_\perp)/2$ and its dual $\tilde{\lambda} = (g_\parallel - g_\perp)/2$, are related to U and $\bar{V}$ by $g_{\parallel,\perp}/a_0 = -U \mp \bar{V}$.

1. Spin sector

Let us first discuss the spin sector. The Hamiltonian (38) describes the competition between two mutually incompatible ordering tendencies favored by the two cosine terms in (38). We thus expect that either the $\vec{\Phi}$ field or its dual $\vec{\Theta}$ gets locked when these terms are relevant. The phase diagram in the spin sector results from a delicate balance between the three interaction terms entering (38). The RG equation associated with the couplings in (38) are given to the one-loop order by [28]

$$\frac{d\tilde{g}_\parallel}{dt} = (N-2)\tilde{g}_\parallel^2 + (N+2)\tilde{g}_\perp^2, \tag{39}$$

$$\frac{d\tilde{g}_\perp}{dt} = 2N \tilde{g}_\parallel \tilde{g}_\perp, \tag{40}$$

where we have rescaled the couplings as $\tilde{g}_{\parallel,\perp} = g_{\parallel,\perp}/4\pi v_F$.

Let us first consider the more interesting situation of an attractive pairing interaction, i.e., when $\bar{V} < 0$. In this case the RG flow always drives the system towards strong coupling and a spin gap opens. The nature of the resulting phase depends on the relative strength of the on-site interaction U and the pairing term. We distinguish between two phases.

$SU(N)$ phase. When $U < \bar{V} < 0$, i.e., when the on-site attraction dominates the pairing term, the RG flow drives the system toward the attractive ray: $g_\parallel = g_\perp = \lambda > 0$. On this line the interacting part of (38) takes the form

$$H_{\text{int}} = \frac{\lambda}{2} \int dx \left[(\partial_x \vec{\Phi})^2 - \frac{1}{\pi^2 a_0^2} \sum_{a<b} \cos(2\pi \vec{\alpha}_{ab} \cdot \vec{\Phi}) \right]. \tag{41}$$

When $\lambda = g_\perp > 0$, the interaction is relevant and a spin gap, $\Delta_\sigma \propto e^{-1/2N\lambda}$, opens. The spin field $\vec{\Phi}$ gets locked in such a way that the cosine terms in (41) are maximal. Using (36) we find that $\vec{\alpha}_{ab} \cdot \vec{\Phi} = \phi_a - \phi_b$, which implies for the flavor fields: $\phi_a - \phi_b = p$, $p \in \mathbb{Z}$. As a consequence the fluctuations of the different flavor densities, $n_a(x)$ in (34), are in phase with each other. In this phase N fermions of different flavors bind together into charge $Q = N$ spin-singlets, forming a compressible fluid. In particular, for $N = 3$, this is the trionic phase discussed in Ref. [29] in which triplets of fermions bind together. This phase is "topologically trivial" (i.e., it has no protected edge states) since it is adiabatically connected to a phase, obtained when $U = -\infty$, where the N-fermion bound states can be described essentially as free spinless fermions.

Although it is not obvious when written in terms of the spin field $\vec{\Phi}$, the Hamiltonian (41) possesses an emergent $SU(N)$ symmetry. To see this, observe that this fixed point corresponds to the pairing V flowing to zero at which the lattice Hamiltonian (30) is clearly $SU(N)$ invariant. Therefore in the whole domain $U < \bar{V} < 0$ an $SU(N)$ symmetry is dynamically enlarged in the low-energy limit.

Dual $\widehat{SU(N)}$ phase. When the pairing term dominates the physics, e.g., when $|\bar{V}| > |U|$, the RG drives the system toward the attractive ray: $g_\parallel = -g_\perp = \lambda > 0$, at which the interacting part of (38) takes the form

$$H_{\text{int}} = \frac{\tilde{\lambda}}{2\pi^2} \int dx \left[(\partial_x \vec{\Theta})^2 - \frac{1}{a_0^2} \sum_{a<b} \cos(2\vec{\alpha}_{ab} \cdot \vec{\Theta}) \right]. \tag{42}$$

As in the previous phase a spin gap, $\Delta_\sigma \propto e^{-1/(2N\tilde{\lambda})}$, opens but this time it is the $\vec{\Theta}$ field that gets locked instead of $\vec{\Phi}$. From (36), we find that this implies: $\theta_a - \theta_b = p\pi$, $p \in \mathbb{Z}$, exactly as in the gapless topological phase discussed in Sec. II B. We

therefore expect that in the dual $\widehat{SU(N)}$ phase the system host protected zero-energy edge states. These edge states transform as a spinor representation of $SO(N)$, as discussed in Sec. II B 2.

The fixed points Hamiltonians (41) and (42) are related by the duality transformation

$$\Omega : \vec{\Theta} \rightleftarrows \pi\vec{\Phi}, \ \Omega^2 = 1. \tag{43}$$

We therefore find that the massless topological phase is *dual* in the sense of (43) to the topologically trivial $SU(N)$ phase. As discussed in Ref. [30] the $SU(N)$ symmetry of (41) translates by the duality (43) into a dual $\widehat{SU(N)}$ symmetry for (42).[3]

Self-Dual phase transition line. When $\bar{V} = U$ there is a quantum phase transition between the two phases. At this point, $g_\perp = 0$, $g_\parallel = \lambda > 0$, and the interacting part of Hamiltonian (38) takes the form

$$H_{\text{int}} = \frac{-\lambda}{2\pi^2 a_0^2}\int dx\left[\sum_{a<b}\cos(2\pi\vec{\alpha}_{ab}\cdot\vec{\Phi}) + \cos(2\vec{\alpha}_{ab}\cdot\vec{\Theta})\right], \tag{44}$$

which is invariant under the duality transformation (43). This is the self-dual line, separating the two dual $SU(N)$ and $\widehat{SU(N)}$ symmetric phases discussed above. As shown by Andrei and Destri [31], the model (44) is integrable and a spin gap $\Delta_\sigma \propto e^{-1/(N-2)\tilde{\lambda}}$ is still present [notice that the spin gap on the self-dual line is parametrically smaller than in both $SU(N)$ and $\widehat{SU(N)}$ phases]. This suggests that the phase transition between the trivial $SU(N)$ phase and the dual $\widehat{SU(N)}$ topological phase is of first order. The model (44) undergoes dynamical symmetry breaking of the dual symmetry (43) with kinks that carry zero modes transforming according to the spinor representation of $SO(N)$. In the particular case of $N = 3$ the model hosts propagating spin-1/2 kinks. This allows us to interpret these spinor kinks as the end modes hosted by the dynamical domain walls between the trivial and topological phases. We will address this result further in Sec. V.

Before ending the description of the phase diagram of (30) let us briefly discuss the simpler situation of a repulsive pairing interaction $\bar{V} > 0$. In this case, if $U > 0$ then the interaction is always irrelevant, and the system remains gapless. When $U < 0$ the interaction is relevant and the system flows toward the strong coupling fixed point associated with the topologically trivial $SU(N)$ phase discussed above.

2. Charge sector

In all phases discussed above the low-energy sector is described by the generalized Luttinger liquid Hamiltonian (37). As far as charge excitations are concerned, the low-energy physics depends only on the nonuniversal Luttinger parameters $K(U, V)$ and $v_c(U, V)$. However, the low-energy excitations in the $SU(N)$ and $\widehat{SU(N)}$ symmetric phases have a different character. Their nature is encoded in the total charge Q and total current J (or zero-mode) spectrum of (37).

In the gapless topological phase, as discussed in Sec. III, we found that, due to the topological nature of a single Kitaev chain and the locking of the spin field $\vec{\Theta}$, the low-energy excitations either change the parity of all the flavors simultaneously or do not change them at all. We then deduced that the total charge and current in the system were given by (20)

$$Q = n, J = mN, \quad Q \pm J \quad \text{even}, \tag{45}$$

where $(n, m) \in \mathbb{Z}$. The fundamental excitation is either a charge $Q = 2$ boson for N even or a composite fermion of charge $Q = 1$ for odd N [27]. In both cases the Fermi momentum P_F is enlarged to $P_F = Nk_F/2$ and $P_F = Nk_F$, respectively.

As seen above, the $SU(N)$ symmetric topologically trivial phase was obtained from the topological $\widehat{SU(N)}$ symmetric one by the duality transformation (43) on the spin bosonic fields $\vec{\Phi}$ and $\vec{\Theta}$. In the charge sector the latter duality translates onto the charge fields

$$N\Theta \rightleftarrows \pi\Phi. \tag{46}$$

We may then deduce the zero mode spectrum of the Luttinger liquid Hamiltonian (37) in this phase

$$Q = nN, J = m, \quad Q \pm J \quad \text{even}. \tag{47}$$

We immediately see that it is the total charge of the system, instead of the current, that is quantized in units of N. The fundamental excitations are $SU(N)$ singlet bound states made of N fermions. They are bosons for N even and fermions for N odd. In both cases the Fermi momentum is that of the lattice fermions, e.g., $P_F = k_F$.[4]

V. THE GAPLESS HALDANE PHASE IN SO(3) SYMMETRIC FERMION CHAINS

In order to illustrate the ideas we laid out above, we now study the model (30) in more detail, focusing on the case of $N = 3$. We consider the system to be at 1/3 filling (one fermion per site) and start by discussing the different limits of the model and the phases that are expected to arise in those limits. A quantitative phase diagram, obtained using DMRG, is presented in Fig. 1 and will be described in greater detail in Sec. V A.

We first consider the case of repulsive on-site interactions, $U > 0$, and vanishing pairing interactions, $V = 0$. In this case, the Hamiltonian has an $SU(3)$ symmetry. In the strong coupling limit, $U \gg t$, we expect the system to be in a Mott phase with a gapped charge sector [32]. The low-energy effective Hamiltonian, obtained by second-order perturbation theory in t/U, is then given by the bilinear-biquadratic spin-1 model

$$H = \sum_i (J_1\vec{S}_i\cdot\vec{S}_{i+1} + J_2(\vec{S}_i\cdot\vec{S}_{i+1})^2), \tag{48}$$

[3] In the terminology used in Ref. [30] the dual fixed point Hamiltonian (41) belongs to the class $\mathcal{A}_I$ and is is associated with the $SO(N)$ symmetry of the problem.

[4] In the classification of Luttinger liquid proposed in Ref. [27] these two phases belong to the classes $\mathcal{A}_I$ and $\mathcal{A}_0$.

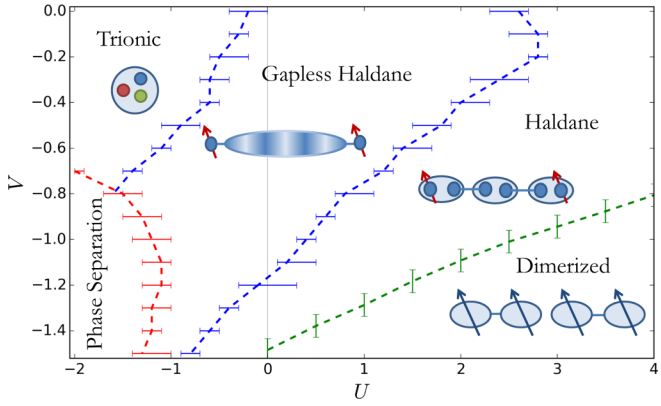

FIG. 1. Phase diagram of the model (30) with $N = 3$ at $1/3$ filling, as a function of the on-site interaction U and nearest neighbor pairing interaction $V < 0$. For repulsive on-site interactions, $U > 0$, a charge gap opens as U is increased and the system goes from the gapless to the gapped Haldane phase. For large enough $|V|$ a transition to the fully gapped dimerized phase is observed. For attractive on-site interactions, $U < 0$, the system undergoes a transition into the trionic phase, in which triplets of fermions bind together into spin singlets. For large attractive U and V the system tends to phase separate. For details on how the phase boundaries are determined, see main text and Appendices A 2, A 3.

where $S^a_i = i\epsilon^{abc} c^\dagger_{i,b} c_{i,c}$ are $S = 1$ operators, and $J_{1,2} = J = 2t^2/U$. The Hamiltonian (48) was studied extensively (see, e.g., Refs. [33,34] and the references therein) and exhibits a rich phase diagram as a function of J_2/J_1. In particular, for $J_1 = J_2$, the model is critical and described by a level-one $SU(3)$ Wess-Zumino-Witten model [28].

When a nonzero V is introduced, the symmetry of the model is reduced to $SO(3)$. In the limit $U \gg t$ and for $V \sim t^2/U$, the low-energy effective Hamiltonian is given by (48) with $J_1 = J$ and $J_2 = J + V$. While for $V > 0$ the system is critical [28], for $V < 0$ it is fully gapped. For $-2J < V < 0$ the system belongs to the Haldane phase with decoupled spin-$1/2$ degrees of freedom localized at its ends, similarly to the AKLT model [35]. For $V < -2J$ a dimerized phase, which breaks translational invariance, is expected.

Going back to the weak coupling limit, i.e., $|U|, |V| \ll t$, we recall the analysis presented in Sec. IV A, which suggested that for $U > 0$ and $V < 0$ the system is in the gapless topological phase. To understand the nature of the topological phase and the end modes in this case, recall that the mean-field description of this phase hosts three Majorana zero modes at each end of the chain, $\gamma_{L(R),a}$. These modes can be combined to form a spin-$1/2$ degree of freedom $S^a_{L(R)} = -\frac{i}{4}\epsilon^{abc}\gamma_{L(R),b}\gamma_{L(R),c}$, similarly to the spin-$1/2$ degrees of freedom in the Haldane phase. In the gapless topological phase, these end modes remain localized at the two ends of the system and cannot couple to one another due to the spin gap in the bulk. Due to the close relation with the Haldane phase, we refer to this phase as the gapless Haldane phase.

Finally, for attractive on-site interactions, $U < 0$, we expect to find a phase transition into the trivial, trionic phase, in which triplets of fermions of different flavors bind together forming an $SU(3)$ singlet.

A. Phase diagram

We describe below the phase diagram of the model, as a function of the on-site interaction strength U, and the nearest neighbor pairing $V < 0$, obtained using DMRG [36] and presented in Fig. 1. In the DMRG calculation, we represent each fermionic flavor as a single chain, and work in the basis $c_{\pm 1} = (c_1 \pm ic_2)/\sqrt{2}$, $c_0 = c_3$, such that $S^3 = n_{+1} - n_{-1}$ is conserved (hereafter, we will denote S^3 by S^z). In agreement with the weak coupling analysis presented in Sec. IV A, we find that as $|V|$ is increased, a finite spin gap opens in the system (see Appendix A 1 a for more details). Hence, all the phases discussed below have a fully gapped spin sector.

1. Mott transition

As discussed above, for large enough $U > 0$ we expect the system to undergo a Mott transition as a charge gap opens. For small $V < 0$ the charge gap opening line separates the gapped and gapless Haldane phases. Note that both phases are expected to host spin-$1/2$ at their edges [see discussion below Eq. (48)]. We shall demonstrate this explicitly for the gapless phase in Sec. V B.

To detect the Mott transition, we calculate the gap to adding a single particle. For a fixed system size N_x we calculate

$$E^{\mathrm{SP}}_{3n=N_x} = E_{3n+1} + E_{3n-1} - 2E_{3n}, \tag{49}$$

where by E_n we denote the ground state energy of a system with n particles. We then extrapolate $E^{\mathrm{SP}}_{3n=N_x}$ to the infinite system size limit. Indeed, we find a finite region in the parameters space, in which for $U < U_c(V)$ the charge sector is gapless. For more details on how $U_c(V)$ is determined see Appendix A 2.

2. Dimerization transition

The strong coupling arguments presented above also suggest that large attractive pairing interactions drive a transition into a dimerized phase. The open boundary conditions used in the simulations always induce some dimerization in the middle region of the system. To identify the transition into the dimerized phase, we calculate the local dimerization $D_i = |\vec{S}_i \cdot \vec{S}_{i+1} - \vec{S}_{i-1} \cdot \vec{S}_i|$. At the dimerization transition, the dimerization in the middle of the chain is expected to decay as a power law $D_{N_x/2} \sim N_x^{-d}$ with an exponent $d = 3/8$ [37].

Performing finite size scaling, we fit $D_{N_x/2}$ to the form given above, extracting the exponent d as a function of V, and identify the phase transition point as the value of V for which the exponent equals $3/8$. For further details and numerical results see Appendix A 3.

3. Trionic phase transition

For large $U < 0$, we expect to find a trionic phase, in which triplets of fermions of different flavors bind together. Although the charge sector in this phase is gapless, similarly to the gapless Haldane phase, the two phases have a qualitatively different spectrum: The trionic phase has a finite gap to one and two fermion excitations, whereas in the Haldane phase both excitations are gapless. In addition, as we explain below, the two phases are topologically distinct. To obtain the phase transition line between these two phases we once again

calculate the single particle gap defined in (49), extrapolating it to the infinite system size limit.

From the field theoretical arguments (see Sec. IV and Ref. [31]), the phase transition between these two phases is expected to be first order. However, while the distinct behaviors in the two phases are readily verified, we find it difficult to verify the nature of the phase transition numerically, due to the small size of the spin gap at the transition point. (Note that the smallness of the gap at the transition point is consistent with the weak coupling analysis above. See Appendix A 4 for results and further discussion).

4. Phase separation

For large $U, V < 0$ the system tends to phase separate, forming clusters of trions. Interestingly, close to the line of the phase transition between the gapless Haldane and the trionic phase the system phase separates into regions in the gapless Haldane phase and a clustered trions region, with localized spin-1/2 modes at the boundaries, in support of the phase transition between the gapless Haldane and the trionic phases being first order (see Appendix A 4 and Fig. 7 therein).

B. Gapless Haldane phase

We now further analyze the region in the phase diagram that we identified as the gapless Haldane phase and discuss its properties. The edges of this phase are expected to support spin-1/2 end modes that can pair into a spin singlet with $S^z = 0$ or a spin triplet with $S^z = 0, \pm 1$. To show the exponential protection of the end modes, we calculate the ground state energy in the total $S^z = 0$ and $S^z = 1$ sectors. As can be seen in Fig. 2(a), this energy splitting decays exponentially in system size. Furthermore, we calculate the local expectation value of S^z in the ground state of the system in the total $S^z = 1$ sector [see Fig. 2(b)]. One can clearly see the localized spins at the two ends of the system (we have checked that S^z near each edge indeed sums to 1/2).

From the discussion in Sec. II, we expect the bare fermions of each flavor to be gapped in the bulk, even though the charge sector is gapless. To see this explicitly for our model, we calculate the two-point correlation function of the fermions (e.g., the c_0 fermions) in the bulk, $\langle c_0^\dagger(0)c_0(x)\rangle$, and find that it decays exponentially with x [see Fig. 2(c)]. Similarly, we consider the correlations of the the charge-1, spinless fermionic operator $\tilde{c} = c_0^\dagger c_1 c_{-1}$, $\langle \tilde{c}^\dagger(0)\tilde{c}(x)\rangle$. This operator changes the fermion parity of all three fermion flavors; therefore, by the arguments of Sec. II, we expect it to have power law correlations in the gapless Haldane phase. These are also plotted in Fig. 2(c). It can be seen that these correlations decay as a power law, with an exponent close to unity. For the ease of presentation, we plot the absolute value of the correlations in Fig. 2(c). We note, however, that the correlations of the $\tilde{c}$ fermions exhibit $3k_F = \pi$ oscillations as expected from the low energy analysis presented in Sec. III.

At this point a natural question to ask is whether the gapless Haldane phase is stable to breaking of the $SO(3)$ symmetry. Given our general heuristic argument we expect the phase to be stable to any perturbation which preserves the $(\mathbb{Z}_2)^3$ symmetry, associated with the conservation of the fermionic

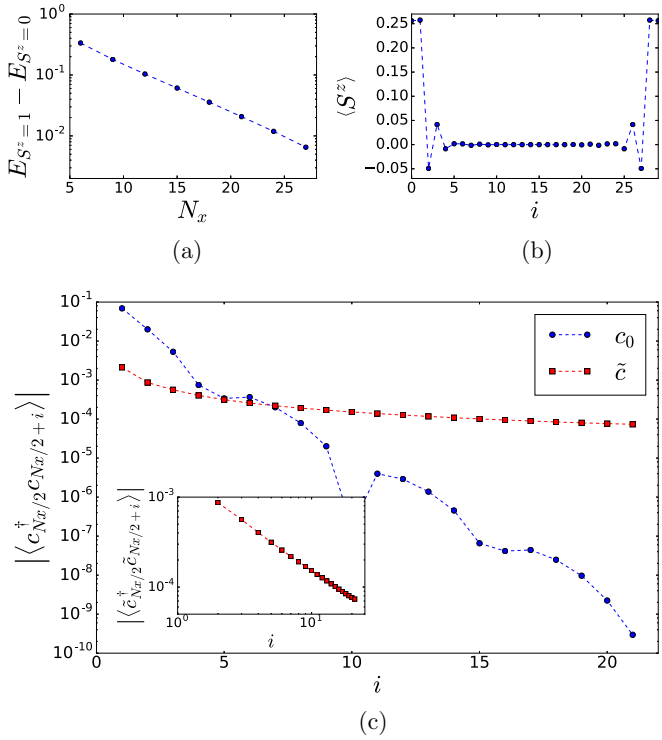

FIG. 2. (a) Energy splitting between the ground states with total $S^z = 1$ and total $S^z = 0$ as a function of the length of the system for $U = 0$, $V = -0.5$ shown on a semilog scale. (b) The expectation value of S^z as a function of position along the chain in the ground states of the system of length $N_x = 30$ sites, model parameters $U = 0$, $V = -0.8$, and total $S^z = 1$. Exponentially localized spin-$\frac{1}{2}$ degrees of freedom can be observed at the ends of the system. (c) Two-point correlations of the bare fermions $\langle c_0^\dagger(i_0)c_0(i_0 + i)\rangle$, and of the charge-1 spinless fermions $\langle \tilde{c}^\dagger(i_0)\tilde{c}(i_0 + i)\rangle$, where $\tilde{c}^\dagger = c_0 c_1^\dagger c_{-1}^\dagger$, plotted in blue (circles) and red (squares), respectively, calculated in the bulk of the system $i_0 = N_x/2$ for a system of size $N_x = 66$ sites and model parameters $U = 0$, $V = -0.8$. The main plot shows the correlations on a semilog scale, while the inset shows the correlations for the charge-1 spinless fermions on a log-log scale. It can be clearly seen that while the former are exponential, the latter are power law as expected.

parities of the three species. For instance, we expect that if a small single-ion anisotropy term, e.g., $D_z \sum_i (S_i^z)^2 = D_z \sum_i (n_{i,+1} - n_{i,-1})^2$, is added to the Hamiltonian (30), the induced coupling between the end modes will be exponential in system size. In Appendix A 5 we present DMRG results, which are consistent with the latter expectation.

VI. CONCLUSIONS

A. Summary of the main results

In this work, we have studied charge-conserving one-dimensional superconductors with generic intrinsic attractive pairing interactions. We presented a general heuristic argument that implies that a system of spinless electrons with no additional symmetries does not support a topological phase with exponentially localized edge states. In contrast, in the presence of additional symmetries, there are distinct topological superconducting phases with exponentially localized

end modes. The properties of the end modes are directly related to those of a corresponding model with explicit mean-field superconducting terms, where the total charge is not conserved.

We examined in detail a situation with $N > 1$ flavors of fermions, in which the fermionic parity of each flavor is separately conserved, resulting in a $(\mathbb{Z}_2)^N$ symmetry. In this case, the system hosts exponentially localized low-energy end modes, which are reminiscent of the Majorana zero-energy bound states found in proximity coupled systems. The stability of these edge states is ensured by the presence of a "flavor gap" due to the attractive pairing interactions and by the very special nature of the gapless modes of the system. Indeed, due to the $(\mathbb{Z}_2)^N$ symmetry we showed that the gapless modes either do not change the fermionic parity of any of the flavors or change them all simultaneously. As a consequence, the coupling between the edges through the gapless bulk modes only lifts the degeneracy between even and odd *total* fermionic parity sectors. The resulting topological degeneracy of the system is $2^N - 1$. We thus found a connection between the nature of the *bulk* low-energy excitations and the existence of a topological phase in a charge conserving system. In particular, these excitations are created by composite bosonic operators with an even charge for N even, and composite fermionic operators with an odd charge and an enlarged Fermi surface at $\pm N k_F$, for N odd. The analysis is readily generalized to other symmetry classes; we discussed the case of a single flavor with time reversal symmetry as an example.

In order to be more explicit, we introduced and studied a simple paradigmatic model which, we believe, captures the essential features of charge conserving topological superconductors. It includes both on-site Hubbard interactions and nearest-neighbor attraction and has a larger $SO(N)$ symmetry. Using field theoretical techniques, we showed that a phase which hosts massless composite bosons and fermions with a large Fermi surface is stabilized. Using the general arguments, we showed that this phase supports zero-energy bound states at its edges, which transform as $SO(N)$ spinors. This gapless topological phase is separated from the trivial phase obtained for a large attractive Hubbard coupling by a quantum phase transition.

Interestingly, the topological phase in the $N = 3$ case is nothing but a gapless analog of the Haldane phase of $S = 1$ spin chains, where the three Majorana zero modes of the topological superconductor can be identified with the localized spin-$1/2$ edge states of the Haldane phase. This phase has gapless charge excitations in the bulk (including fermionic excitations with a unit charge). The edge states are protected either by the $SO(3)$ symmetry, or more generally by the separate conservation of the parity of each of the three fermion flavors. Upon opening a charge gap, this phase becomes the conventional (insulating) $S = 1$ spin chain.

Finally, we identify the transition between the gapless Haldane phase and the trivial trionic phase with the self-dual transition found in an integrable model by Andrei and Destri [31]. This naturally explains the degeneracy associated with the kinks between the two phases, that was noted in Ref. [31], as domain walls between two topologically distinct phases that carry spin-$1/2$ zero modes.

B. Future directions

We end with some remarks about open questions and comment on possible experimental realizations of the phases discussed in this work. An important question that we have not addressed here is the effect of impurities on the topologically nontrivial gapless phases. For $N = 2$, it is known that the topological phase is robust for sufficiently weak disorder that preserves the symmetry [12,18]. If the disorder is too strong, however, the system becomes localized, and its topological properties are lost. It is interesting to ask whether the same occurs for the $N > 2$ phases.

A related question pertains to the properties of the Mott insulating phase proximate to the topological gapless phase. For $N = 2$, this phase is a trivial insulator; in contrast, for $N = 3$, it is the symmetry-protected Haldane phase. We speculate that the Mott insulating phases for $N > 3$ are symmetry-protected gapped phases which can be viewed as generalized Haldane phases; this remains to be investigated in detail.

We comment briefly on possible experimental realizations of the $N > 1$ phases. The $N = 2$ phase can arise in superconducting quantum wires with spin-orbit coupling [9,12,18]. Similarly, phases with $N > 2$ modes can arise in quantum wires with multiple subbands, similar to the system described in Ref. [5]. As long as the wires are sufficiently clean, and the potential landscape along the wire is slowly varying on the scale of the Fermi momentum, the different Fermi momenta of the different subbands guarantee that single electrons cannot scatter from one subband to the other at low energies. In contrast, pairs of electrons with opposite momenta can scatter between subbands. This gives an approximate $(Z_2)^N$ symmetry that corresponds to the separate conservation of the fermion parity of every subband. In principle, the edge of the system breaks this $(Z_2)^N$ symmetry, since it breaks translational symmetry, and thus it allows single electron scattering between subbands. However, if the confining potential at the end of the wire is sufficiently smooth, such scattering is exponentially suppressed in the gradient of the potential; see, e.g., Refs. [6,38]. Thus, near-zero energy states appear at the ends of the system. The quasizero modes manifest themselves in an enhanced low-energy single-electron tunneling density of states at the ends. For N even, the bulk is gapped for single electrons, whereas for N odd there is no bulk gap for single electron excitations.[5] Nevertheless, we expect the bulk tunneling density of states to be suppressed at low bias voltage due to interaction effects. Such systems deserve a more detailed investigation that we leave to future studies. Finally, a different possible realization of the $N > 2$ phases is in systems of cold alkaline rare earth Fermi gases that have a high hyperfine degeneracy and an approximate SU(N) symmetry; see, e.g., Ref. [39] and the references therein.

ACKNOWLEDGMENTS

E.B. acknowledges support from the European Research Council (ERC) under the European Union Horizon 2020

[5]These are "composite" excitations that involve adding an electron to one mode and creating particle-hole pairs in all the other modes, as described in Sec. II B 1.

Research and Innovation Programme (Grant Agreement No. 639172), from a Minerva ARCHES prize, and from CRC 183 of the Deutsche Forschungsgemeinschaft. We acknowledge the hospitality of KITP at UCSB, which is supported by NSF Grant No. PHY-1125915. P.A. wants to thank the Weizmann Institute for its kind hospitality while this work started.

APPENDIX: ADDITIONAL NUMERICAL RESULTS

1. Further analysis of the gapless Haldane phase

In this appendix, we consider the spin and the charge sectors in the gapless Haldane phase, showing that a finite gap opens in the former while the latter remains gapless.

a. Spin gap

Below, we calculate the spin gap in the bulk as $|V|$ is increased. To this end, we calculate the energy gap to $S^z = +2$ excitations, as we expect the gap to $S^z = +1$ excitations to vanish for a system with open boundary conditions due to the spin-1/2 end modes. More specifically, we calculate

$$\Delta_\sigma = \lim_{N_x\to\infty} [E_{(n+1,n,n-1)} - E_{(n,n,n)}]_{n=\frac{N_x}{3}}, \qquad \text{(A1)}$$

where we denote by $E_{(n_{+1},n_0,n_{-1})}$ the ground state energy of a system with $n_{+1,0,-1}$ particles of flavor $+1$, 0, and -1, respectively. The spin gap, Δ_σ, for $U = 0$ as a function of V is shown in Fig. 3(a). It can be seen that, indeed, a finite spin gap opens as $|V|$ is increased.

b. Charge Luttinger parameter

To verify that the charge sector is indeed gapless in the region we identify as the gapless Haldane phase, we calculate the charge Luttinger parameter numerically. To this end, we first calculate the energy of the first excited state in the $S_z = 1$ sector as a function of system size. Assuming the spin sector is gapped, the energy of the first excited state is given by $\pi v_c/L$, allowing us to extract the value of the charge velocity v_c. (In practice, since the spin gap for small values of V is small, for small systems sizes the spin sector will appear gapless with the corresponding velocity v_σ, and the first excited state will be given by $\min(\pi v_c/L, \pi v_\sigma/L)$, allowing us to obtain only a lower bound for v_c). Next, we calculate the energy gap to adding a single particle of each species, as a function of system size, i.e.,

$$\begin{aligned} &E_{3n+3} + E_{3n-3} - 2E_{3n} \\ &= \frac{1}{L}\frac{\pi v_c}{2K}[(3n+3)^2 + (3n-3)^2 - 2(3n)^2] \\ &= \frac{1}{L}\frac{9\pi v_c}{NK}. \end{aligned} \qquad \text{(A2)}$$

Here $E_{3n} = E_{(n,n,n)}$, with the total number of particles $3n$ equal to the number of lattice sites N_x, and $N = 3$ is the number of flavors. (We add a single particle of each species to avoid excitations of the spin sector at small values of V, when the spin gap is small.) The extracted charge Luttinger parameter is plotted in Fig. 3(b).

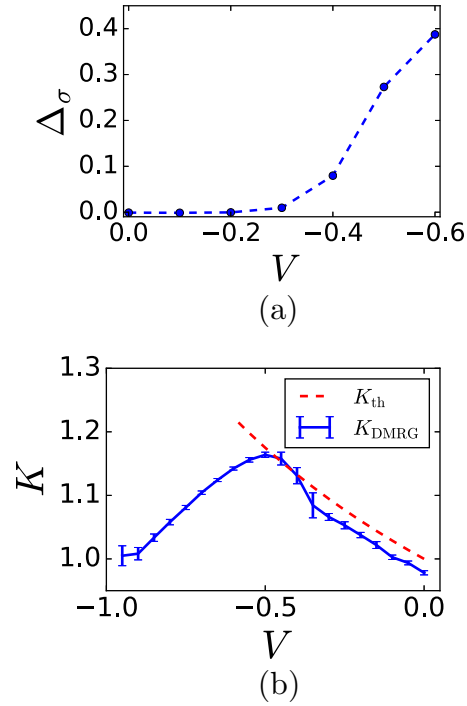

FIG. 3. (a) The spin gap, Δ_σ [defined in Eq. (A1)] and (b) the charge Luttinger parameter, K, for $U = 0$ as a function of V. (a) For $V \lesssim -0.3$ a finite spin gap is observed. (b) The Luttinger parameter in the charge sector obtained numerically (blue solid line), compared to the analytical value obtained using weak coupling analysis (red dashed line).

The analytical value of K obtained from weak coupling analysis (see Sec. IV A in the main text), given by $K = (1 + \bar{V}/\pi v_F)^{-1/2}$ for $U = 0$, is shown on the same plot for comparison. The critical value of the charge Luttinger parameter K, at which a charge gap is expected to open, is equal to 2/3. Although we observe the general trend of the decrease in K with increasing $|V|$ numerically (for $V \lesssim -0.5$), we could not obtain the value of K close to the charge gap opening point with good enough precision to validate this.

2. Determining the phase boundary of the gapless Haldane phase

To obtain the phase boundary between the gapless and the fully gapped Haldane phases (i.e., the Mott transition point), we calculate the gap to adding a single particle as a function of U for each value of V and obtain the critical value of U, $U_c(V)$, for which this gap becomes finite. More specifically, we calculate $E^{\rm SP}_{3n}$ [see Eq. (49) in the main text] for different system sizes up to $N_x = 48$ sites (where we take the total number of particles $3n$ to be equal the number of lattices sites N_x) and extrapolate it to the infinite system size limit, denoting $E^{\rm SP} = \lim_{N_x\to\infty} E^{\rm SP}_{3n}$. (The single particle gap is calculated in the $S^z = 0$ sector, i.e., we calculate $E_{(n,n+1,n)} + E_{(n,n-1,n)} - 2E_{(n,n,n)}$.)

Numerically, it is difficult to obtain the charge gap opening point directly from the function $E^{\rm SP}(U)$. Instead, we consider

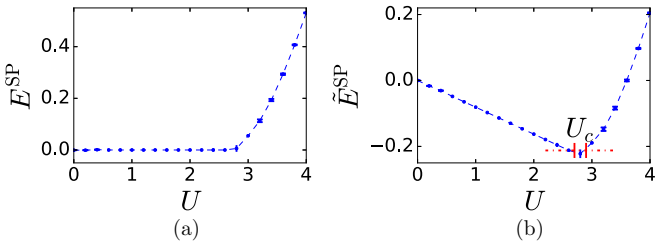

FIG. 4. The (a) single particle gap, $E^{SP}(U)$, and (b) the transformed function $\tilde{E}^{SP}(U)$ [see Eq. (A3)] for $V = -0.2$. The transformed function exhibits a minimum at the point where the single particle gap becomes finite. The error in U_c is estimated from the error in $E^{SP}(U_c)$ as depicted in the figure.

the function

$$\tilde{E}^{SP}(U) = E^{SP}(U) - E^{SP}(U=0) - \frac{E^{SP}(U=U_0) - E^{SP}(U=0)}{U_0} U, \quad \text{(A3)}$$

where $U_0 > U_c$. (The value of U_0 is somewhat arbitrary and we choose it such that $E^{SP}(U = U_0) > 0.2$.) This function has an extremum point at U_c, making it easier to identify numerically (see Fig. 4).

3. Dimerization transition

As was mentioned in the main text, we find that large attractive pairing interactions drive a transition into a dimerized phase. To obtain the point of the phase transition into the dimerized phase, we calculate the local dimerization $D_i = |\vec{S}_i \cdot \vec{S}_{i+1} - \vec{S}_{i-1} \cdot \vec{S}_i|$. At the dimerization transition, the dimerization in the middle of the chain is expected to decay as a power law $D_{N_x/2} \sim N_x^{-d}$ with an exponent $d = 3/8$. Performing finite size scaling, we fit $D_{N_x/2}$ to a power law [see Fig. 5(a)], extracting the exponent d as function of V. We then identify the phase transition point as the value of V for which the exponent equals $3/8$ [see Fig. 5(b)].

4. Phase transition between the trionic and gapless Haldane phase and phase separation

As was discussed in Sec. IV A, the phase transition between the trionic phase and the gapless Haldane phase is expected to be first order, with a finite spin gap at the transition. In Fig. 6, we plot the spin gap as function of U for $V = -0.6$ and observe it approaching zero at the phase transition point. We attribute this to the fact that, in the weak coupling limit, the spin gap along the phase transition line is expected to be parametrically smaller than deep in either phase, as was also mentioned in Sec. IV A. To estimate the magnitude of the spin gap expected at the phase transition, one may use the one-loop RG equations and the results for the phase transition point obtained from DMRG. For instance, for $V = -0.6$, the phase transition is observed at $U_c \sim -1$, giving a spin gap $\Delta_\sigma \sim 0.5 \times 10^{-3}$. Going to larger system sizes, and larger bond dimension used in the DMRG calculation, would perhaps allow one to resolve the finite size of the gap at the transition.

As was mentioned in the main text, for large $U, V < 0$ the system tends to phase separate. Close to the line of the phase transition between the gapless Haldane and the trionic phase the system phase separates into regions in the gapless Haldane phase and a clustered trions region, with localized spin-1/2 modes at the boundaries as can be seen in Fig. 7. This supports the statement that the phase transition between the gapless Haldane and the trionic phases is indeed first order.

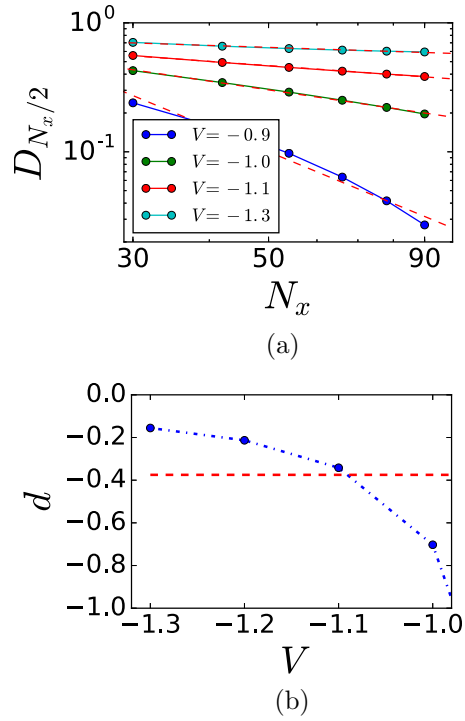

FIG. 5. (a) The local dimerization at the central bond, as a function of system size, for $U = 2$ and varying V. For each value of V, a fit to a power law is plotted with a red dashed line. (b) The exponent, extracted from the fit of the dimerization at the central bond as a function of system size to a power law, as a function of V. The red dashed line corresponds to $d = 3/8$—the exponent expected at the dimerization transition.

5. Stability to $SO(3)$ symmetry breaking

As discussed in the main text, we expect the topological phase to be stable to breaking of $SO(3)$ symmetry, as long as the $(\mathbb{Z}_2)^3$ symmetry, associated with the conservation of the fermionic parities of the three species, is preserved. To test this, we add a single ion anisotropy term $\sum_i D_z (S_i^z)^2$ to the

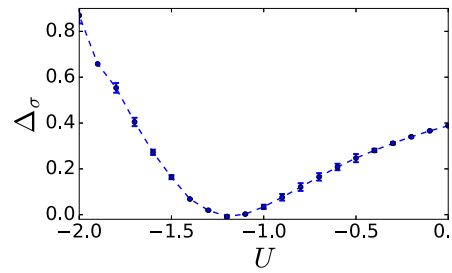

FIG. 6. The spin gap, defined in Eq. (A1), for $V = -0.6$, as a function of U. The vanishingly small gap observed at the phase transition point numerically is consistent with the weak coupling analysis.

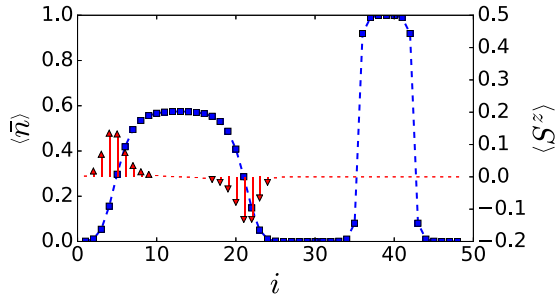

FIG. 7. Expectation value of the average density $\bar{n} = (n_{+1} + n_0 + n_{-1})/(3N_x)$ (blue squares) and the spin density (red arrows) in the phase separated regime, for $V = -1.5$, $U = -1.6$. A coexistence between the topological gapless Haldane phase, featuring localized spin-1/2 modes at its boundaries, and the trivial trionic phase (with the trions bunching together due to the large attractive pairing interactions), can be observed.

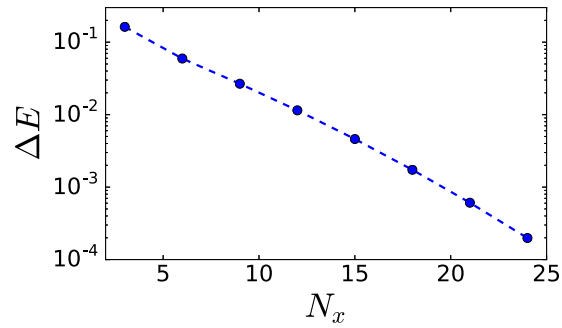

FIG. 8. The energy splitting between the states $|S_L^z = \frac{1}{2}, S_R^z = \frac{1}{2}\rangle$ and $|S_L^z = \frac{1}{2}, S_R^z = -\frac{1}{2}\rangle$, in the presence of a single ion anisotropy term $\sum_i D_z (S_i^z)^2$, for $D_z = 0.4$, as a function of system size.

model (30) and study the coupling between the end modes. To this end, we calculate the energy splitting between the states $|S_L^z = \frac{1}{2}, S_R^z = \frac{1}{2}\rangle$ and $|S_L^z = \frac{1}{2}, S_R^z = -\frac{1}{2}\rangle$ as a function of system size. (To induce the desired polarization at each end, we apply a small Zeeman field at both ends of the chain.) As can be seen in Fig. 8, we find the energy splitting, and hence the coupling between the end modes, to be exponential in system size.

[1] J. Alicea, Rep. Prog. Phys. **75**, 076501 (2012).
[2] C. Beenakker, Annu. Rev. Condens. Matter Phys. **4**, 113 (2013).
[3] M. Leijnse and K. Flensberg, Semicond. Sci. Technol. **27**, 124003 (2012).
[4] L. Fidkowski, R. Lutchyn, C. Nayak, and M. Fisher, Phys. Rev. B **84**, 195436 (2011).
[5] J. Sau, B. Halperin, K. Flensberg, and S. Das Sarma, Phys. Rev. B **84**, 144509 (2011).
[6] J. Ruhman, E. Berg, and E. Altman, Phys. Rev. Lett. **114**, 100401 (2015).
[7] C. L. Kane, A. Stern, and B. I. Halperin, Phys. Rev. X **7**, 031009 (2017).
[8] O. A. Starykh, D. L. Maslov, W. Häusler, L. I. Glazman, and Glazman, in *Low-Dimensional Systems*, edited by T. Brandes (Springer Berlin Heidelberg, Berlin, Heidelberg, 2000), pp. 37–78.
[9] J. Sun, S. Gangadharaiah, and O. A. Starykh, Phys. Rev. Lett. **98**, 126408 (2007).
[10] J. Ruhman, E. G. Dalla Torre, S. D. Huber, and E. Altman, Phys. Rev. B **85**, 125121 (2012).
[11] C. V. Kraus, M. Dalmonte, M. A. Baranov, A. M. Läuchli, and P. Zoller, Phys. Rev. Lett. **111**, 173004 (2013).
[12] A. Keselman and E. Berg, Phys. Rev. B **91**, 235309 (2015).
[13] F. Iemini, L. Mazza, D. Rossini, R. Fazio, and S. Diehl, Phys. Rev. Lett. **115**, 156402 (2015).
[14] C. Chen, W. Yan, C. Ting, Y. Chen, and F. Burnell, Phys. Rev. B **98**, 161106 (2018).
[15] N. Kainaris, R. A. Santos, D. B. Gutman, and S. T. Carr, Fortschr. Phys. **65**, 1600054 (2017).
[16] N. Kainaris, S. T. Carr, and A. D. Mirlin, Phys. Rev. B **97**, 115107 (2018).
[17] T. Scaffidi, D. E. Parker, and R. Vasseur, Phys. Rev. X **7**, 041048 (2017).
[18] N. Kainaris and S. T. Carr, Phys. Rev. B **92**, 035139 (2015).
[19] R. A. Santos, D. B. Gutman, and S. T. Carr, Phys. Rev. B **93**, 235436 (2016).
[20] H.-C. Jiang, Z.-X. Li, A. Seidel, and D.-H. Lee, Sci. Bull. **63**, 753 (2018).
[21] S. R. White, Phys. Rev. Lett. **69**, 2863 (1992).
[22] S. R. White, Phys. Rev. B **48**, 10345 (1993).
[23] M. Yamanaka, M. Oshikawa, and I. Affleck, Phys. Rev. Lett. **79**, 1110 (1997).
[24] J. Ruhman and E. Altman, Phys. Rev. B **96**, 085133 (2017).
[25] A. Altland and M. R. Zirnbauer, Phys. Rev. B **55**, 1142 (1997).
[26] A. Y. Kitaev, Phys. Usp. **44**, 131 (2001).
[27] P. Azaria, Phys. Rev. B **95**, 125106 (2017).
[28] C. Itoi and M.-H. Kato, Phys. Rev. B **55**, 8295 (1997).
[29] P. Lecheminant, P. Azaria, E. Boulat, S. Capponi, G. Roux, and S. White, I. J. Mod. Phys. E **17**, 2110 (2008).
[30] E. Boulat, P. Azaria, and P. Lecheminant, Nucl. Phys. B **822**, 367 (2009).
[31] N. Andrei and C. Destri, Nucl. Phys. B **231**, 445 (1984).
[32] R. Assaraf, P. Azaria, M. Caffarel, and P. Lecheminant, Phys. Rev. B **60**, 2299 (1999).
[33] U. Schollwöck, T. Jolicœur, and T. Garel, Phys. Rev. B **53**, 3304 (1996).
[34] H.-H. Tu, G.-M. Zhang, and T. Xiang, Phys. Rev. B **78**, 094404 (2008).
[35] I. Affleck, T. Kennedy, E. H. Lieb, and H. Tasaki, Phys. Rev. Lett. **59**, 799 (1987).
[36] Calculations were performed using the ITensor Library, http://itensor.org/.
[37] N. Chepiga, I. Affleck, and F. Mila, Phys. Rev. B **93**, 241108 (2016).
[38] G. Kells, D. Meidan, and P. W. Brouwer, Phys. Rev. B **86**, 100503 (2012).
[39] M. A. Cazalilla and A. M. Rey, Rep. Prog. Phys. **77**, 124401 (2014).